NOVEL OPTIMIZED OPERATION OF WIND SYSTEM BASED SHUNT ACTIVE FILTER (W-SAF) TO MITIGATE THE CURRENT HARMONICS FOR ENERGY CONSERVATION

G. VIJAYAKUMAR[1], C. KARTHIKEYAN[1], V. RAVI[1]

[1]Assistant Professor, K.S.R. College of Engineering, Thiruchengode – 637 215, India
vijayakumargovind@yahoo.com, karthikeya@yahoo.com, ervravi@gmail.com

Abstract: *The paper presents the concept of wind power generation system inverter as SAF under balanced and un-balanced conditions. PV based systems are practically inactive during the night time, Because of the system cannot conserve the energy on the night time. During the night time, the PV-SAF provides only the compensation for the reactive power disturbance through the battery bank. The reference currents extract by the Fuzzy logic controller based instantaneous active and reactive power (p-q) strategy. When the supply voltages are balanced and sinusoidal, then all controllers converge to the same compensation characteristics. However, when the supply voltages are distorted and/or un-balanced sinusoidal, these control strategies result in different degrees of compensation in harmonics. The p-q control strategy with PI controller is unable to yield an adequate solution when source voltages are not ideal. Extensive simulations were carried out; simulations were performed with balance, unbalanced and non sinusoidal conditions. Simulation results validate the dynamic behavior of Fuzzy logic controller over PI controller.*
Keywords: *Wind, Shunt Active Filter (W-SAF), conservation, P-Q Control, Fuzzy .*

1. Introduction

Recently, the increased numbers of sensitive loads such as computers, medical equipment, devices for automation and devices in Information Technology have been integrated into the electrical power distribution system. These devices, which are operated continuously during 24 hours period, demand highly reliable input power supply and voltage stability. Supplying unreliable power supply to these devices brings severe losses to the domestic and industrial customers. On the other hand, the growth of non-linear loads like devices with switching power supplies have increased the Electro Magnetic Interference (EMI) problems, real and reactive power losses which causes harmonics, voltage sag/voltage swell and flicker phenomena on the line voltage. The requirements for the power quality become more and more important to keep the safety of electrical devices and customer satisfaction.

The SAF which is connected in shunt with the sensitive loads or a distribution system injects the real and reactive power demanded by the load during the compensation. Especially, the cost of the DC link energy storage capacitor remains high. The use of small capacitors provides a fraction of the energy stored in the DC-link capacitor, which makes it almost impossible for the SAF to compensate load demands. The SAF uses the energy stored in the DC-link capacitor during the compensation. Hence, the DC-link voltage is decreasing during the compensation. For a given DC-link voltage, the output voltage of the SAF is limited by the maximum modulation index. It degrades the capability of the SAF in mitigating harmonics. In addition, the SAF supported by the DC-link capacitor consume more power from the utility distribution system for the continuous compensation. Taking these aspects into account, renewable power generation system integrated with SAF is proposed in this work.

Instantaneous active and reactive theory (p-q theory) was introduced by H. Akagi, Kawakawa, and Nabae in 1984 [1], Since then, many scientists [2-5] and engineers made significant contributions to its modifications in three-phase four-wire circuits and its applications to power electronic equipment. The p-q theory [6] based on a set of instantaneous powers defined in the time domain. No restrictions are imposed on the voltage and current waveforms, and it can be applied to three phase systems with or without neutral wire for three phase generic voltage and current waveforms. Thus it is valid not only in the steady state but also in the transient state. p-q theory needs additional PLL circuit for synchronization so p-q method is frequency variant.

Received on: 30.07.2013
Accepted on: 04.10.2014

Fuzzy logic controllers have generated a great deal of interest in various applications and have been introduced in the power-electronics. The advantages of fuzzy logic controllers over the conventional PI controller are that they do not need an accurate mathematical model; they can work with imprecise inputs, can handle nonlinearity, and may be more robust than the conventional PI controller. The Mamdani type of fuzzy controller used for the control of SAF gives better results compared with the PI controller, but it has the drawback of a larger number of fuzzy sets and 49 rules [7]. Though several control techniques and strategies had developed but still performance of filter in contradictions [8], these became primarily motivation for the current paper. Present paper focusing the performance of the on fuzzy controller, in addition to developed a filter with instantaneous active and reactive power (p-q) method which is prominent one to analyze the performance of filter under different main voltages. On observing fuzzy controller shows some superior performance over PI controller. To validate current THD observations, Extensive simulations were performed and the detailed simulation results are included.

2. Configuration of Three-Phase W-Saf

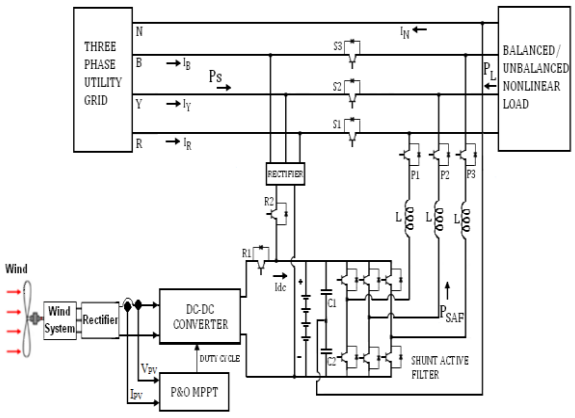

Figure 1. Circuit topology of the three-phase W-SAF

The power circuit of the proposed wind system based SAF topology namely W-SAF is presented. The W-SAF is designed to compensate the current disturbance at the load side. It is also deigned to inject the real power generated by the Wind system to load on both the daytime and night time. When the power generation on the Wind system is less than the load demand, then the proposed coordinating logic connects the output of the three-phase rectifier in parallel with the DC-link to share the load demand with the Wind system. The W-SAF consists of wind turbine, PMSG, controlled rectifier, DC-DC boost converter, DC energy storage unit, three-phase VSI, LC filters and semiconductor switches S_1, S_2, S_3, P_1, P_2, P_3 and R_1, R_2. The power circuit topology of the proposed three-phase W-SAF is shown in Figure 1. When the service grid voltage is normal, then the semiconductor switches S_1, S_2, S_3 are turned ON and R_1, R_2 are turned OFF. When the disturbance occurs or the Wind system generates excessive power than the load demand, the switch R_1 is activated and the SAF inverter supplies power to the load from the battery bank or Wind system.

Table 1. Control signals for S_1, S_2, S_3, P_1, P_2, P_3 and R_1, R_2.

Mode	Control Signals					
	S_1	S_2	S_3	P_1	P_2	P_3
Compensation	1	1	1	1	1	1
UPS / Energy Conservation	0	0	0	1	1	1

Table 2. Battery charge control

Condition	Control Signals		Battery Charging Unit
	R_1	R_2	
$P_{WIND} \geq P_L$	1	0	Wind system
$P_{WIND} < P_L$	1	1	Wind system & Rectifier

The proposed three-phase W-SAF operates in two modes as: 1) SAF compensation mode and 2) UPS / Energy conservation mode. In first mode, when SAF detects deviation in the current, then the SAF enters into compensation mode. Three-phase AC supply are injected in shunt with desired magnitude, phase angle and wave shape for the compensation. The series switches S_1, S_2, S_3 and R_1 are turned ON. The SAF starts to mitigate the harmonics as well as charge the capacitor to maintain the constant magnitude. In second mode, when the interruption occurs in the supply current, the SAF enters into UPS mode. During this mode of operation three-phase W-SAF are connected in parallel with the load to provide an uninterruptable power supply through the battery bank on both daytime and night time. The switches S_1, S_2, S_3 are turned OFF and the switches P_1, P_2 and P_3 are turned ON. The SAF starts to mitigate the interruptions as soon as it detects the interruption. The SAF transfer the wind power to the AC load through the three-phase VSI.

The operation performance of the inverter is feed the excess energy generated by the wind system to load. When the wind system generated power is more, the switch R_1 is turned ON and the switch R_2 is turned OFF. Then, the power generated on the wind system can be fed directly to the load. The Battery charging operation of the W-SAF is subdivided into two categories: They are, (1) $P_{WIND} \geq P_L$, when the wind system generates excessive or equal real power to the load demand, then the SAF enters into energy conservation mode. The system aims to transfer the power generated on the wind system to the AC load through the three-phase VSI. The excessive power generation on the wind system, turns ON the switch R_1 and turns OFF the switch R_2. During this mode, the switches S_1, S_2, S_3 are turned OFF and the switches P_1, P_2 and P_3 are turned ON as presented in Table 2. (2) $P_{WIND} < P_L$, When the power generation on the wind power system is lower than the load demand, the coordinating logic depicted in the Table 2, configures the three-phase rectifier output in parallel with the wind output by closing the semiconductor switches R_1 and R_2 to share the load demand. In this mode, the proposed W-SAF disconnects the utility grid from load and to

perform the inverter operation to feed the power available in the DC-link to load.

3. Instantaneous Active and Reactive Power (P-Q) Method

The control algorithm block diagram for p-q method is depicted in Fig.2. The three-phase source voltages (v_{sa}, v_{sb}, v_{sc}) and load currents (i_{La}, i_{Lb}, i_{Lc}) in the a-b-c coordinates are algebraically transformed to the α-β co-ordinates using Clarke's transformation. In this method [9], a set of voltages (v_a, v_b, v_c) and currents (ia, ib, ic) from phase coordinates are first transferred to the 0αβ coordinates using Clark transformation is given by,

$$\begin{matrix} i_0 \\ i_d \\ i_q \end{matrix} = \frac{1}{v_{\alpha\beta}} \begin{matrix} 1 & 0 & 0 \\ 0 & \cos\theta & \sin\theta \\ 0 & -\sin\theta & \cos\theta \end{matrix} \begin{matrix} i_0 \\ i_\alpha \\ i_\beta \end{matrix} \quad (1)$$

Each current component (id, iq) has an average value or dc component and an oscillating value or ac component

$$i_d = \imath_d + \imath_d$$

$$i_q = \imath_q + \imath_d \quad (2)$$

In this method, only the currents magnitudes are transformed and p–q formulation is only performed on the instantaneous active id and instantaneous reactive iq components. If the d axis has the same direction as the voltage space vector v, then the zero-sequence component of current remains invariant. Therefore, the id–iq method may be expressed as follows:

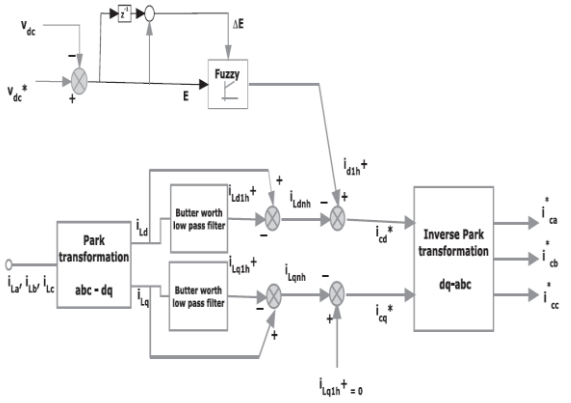

Figure 2. Reference current extraction using fuzzy controller

$$\begin{matrix} i_d \\ i_q \\ i_0 \end{matrix} = \frac{1}{v_{\alpha\beta}} \begin{matrix} v_\alpha & v_\beta & 0 \\ -v_\beta & v_\alpha & 0 \\ 0 & 0 & v_{\alpha\beta} \end{matrix} \begin{matrix} i_0 \\ i_\alpha \\ i_\beta \end{matrix} \quad (3)$$

In this strategy, the source must deliver the constant term of the direct-axis component of load (for harmonic compensation and power factor correction). The reference source current will be calculated as follows:

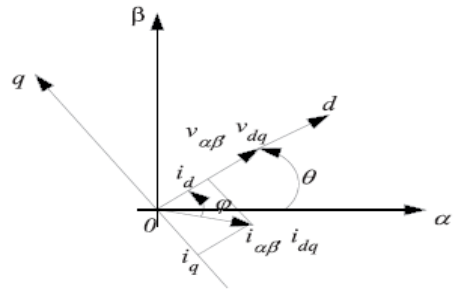

Figure 3. Instantaneous voltage and current vectors.

$$i_{sd} = \imath_{Ld} \; ; \; i_{sq} = i_{s0} = 0 \quad (4)$$

$$i_{Ld} = \frac{v_\alpha i_{L\alpha} + v_\beta i_{L\beta}}{v_{\alpha\beta}} = \frac{P_{L\alpha\beta}}{\overline{v_\alpha^2 + v_\beta^2}} \quad (5)$$

The dc component of the above equation will be

$$\imath_{Ld} = \left(\frac{P_{L\alpha\beta}}{v_{\alpha\beta}}\right)_{dc} = \left(\frac{P_{L\alpha\beta}}{\overline{v_\alpha^2 + v_\beta^2}}\right)_{dc} \quad (6)$$

Where the subscript ''dc'' means the average value of the expression within the parentheses. Since the reference source current must to be in phase with the voltage at the PCC (and have no zero-sequence component), it will be calculated (in a–b–0 coordinate) by multiplying the above equation by a unit vector in the direction of the PCC voltage space vector (excluding the zero-sequence component):

$$i_{sref} = \imath_{Ld} \frac{1}{v_{\alpha\beta}} \begin{matrix} v_\alpha \\ v_\beta \\ 0 \end{matrix} \quad (7)$$

$$\begin{matrix} i_{s\alpha ref} \\ i_{s\beta ref} \\ i_{s0ref} \end{matrix} = \frac{P_{L\alpha\beta}}{v_{\alpha\beta}}_{dc} \frac{1}{v_{\alpha\beta}} \begin{matrix} v_\alpha \\ v_\beta \\ 0 \end{matrix} \quad (8)$$

$$\begin{matrix} i_{s\alpha ref} \\ i_{s\beta ref} \\ i_{s0ref} \end{matrix} = \frac{P_{L\alpha\beta}}{\overline{v_\alpha^2 + v_\beta^2}}_{dc} \frac{1}{v_{\alpha\beta}} \begin{matrix} v_\alpha \\ v_\beta \\ 0 \end{matrix} \quad (9)$$

Reference currents are extracted with id–iq method using FLC which is shown in Fig. 3. In order to maintain DC link voltage constant FLC branch is added to the d axis in d–q frame to control the active current component. The FLC controls this small amount of active current and then the current controller regulates this current to maintain the DC link capacitor voltage.

The reference signals thus obtained are compared with the actual compensating filter currents in a hysteresis comparator, where the actual current is forced to follow the reference and provides instantaneous compensation by the SAF on account of its easy implementation and quick prevail over fast current transitions. This consequently provides switching signals to trigger the IGBTs inside the inverter. Ultimately, the filter provides necessary compensation for harmonics in the source current and reactive power unbalance in the system.

Fig. 2. and Fig. 3. shows the control diagram for shunt active filter and harmonic injection circuit. On owing load currents id and iq are obtained from park transformation then they are allowed to pass through the high pass filter to eliminate dc components in the nonlinear load currents. Filters used in the circuit are Butterworth type and to reduce the influence of high pass filter an alternative high pass filter can be used in the circuit. It can be obtained through the low pass filter (LPF) of same order and cut-off frequency simply difference between the input signal and the filtered one, which is clearly shown in Fig. 4. Butterworth filters used in harmonic injecting circuit have cut-off frequency equal to one half of the main frequency (fc = f/2), with this a small phase shift in harmonics and sufficiently high transient response can be obtained.

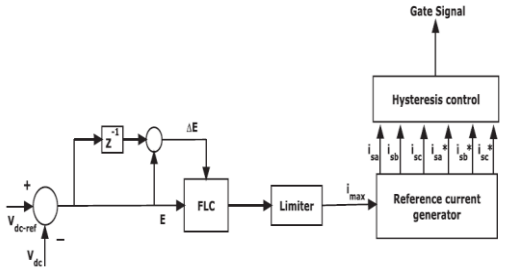

Figure 4. Proposed fuzzy system.

4. Wind Site Selection and Modelling

Table 3 shows the average wind speed at Erode district, Tamil Nadu, India for a period of 15days month. These data are collected from Tamil Nadu Agricultural University, Coimbatore (TNAU, 2013) to estimate the possible output of the wind system. From Table 3, it is observed that the location is well endowed with wind resources, which favors the use of wind conversion system in the selected area.

Table 3 - Erode weather data

Date	Air Temp. (^{0}C)		Wind Speed (kmph)
	Max	Min	
01.06.2013	30.6	23.5	4.71
02.06.2013	30.1	23.8	2.02
03.06.2013	31.9	21.9	2.23
04.06.2013	30.8	23.7	3.47
05.06.2013	31.7	22.3	2.69
06.06.2013	32.0	20.1	2.13
07.06.2013	31.9	20.4	2.59
08.06.2013	30.9	19.2	2.99
09.06.2013	30.5	20.2	2.88
10.06.2013	32.5	21.4	2.17
11.06.2013	31.5	21.4	2.42
12.06.2013	32.9	21.3	2.06
13.06.2013	32.4	21.1	2.21
14.06.2013	32.2	23.0	2.39
15.06.2013	32.7	21.0	3.09
Average	**31.1**	**20.3**	**2.64**

4.1 Wind Turbine Model

The wind mills used in the past are builted with the vertical axis structure. This type is used in small scale installations [10]. The common design of modern turbines is based on the horizontal axis structure. The horizontal axis turbines mounted on the tower, harness more energy than the vertical axis turbines. The kinetic energy in air mass 'm' moving with wind speed V and the power in the moving air is proportional to the flow rate of kinetic energy per second and it can be expressed as

$$Kinetic\ Energy = \frac{1}{2}\ mV^2 \quad (10)$$

$$Power(P) = \frac{1}{2}\ mass\ flow\ rate\ of\ air/second\ V^2 \quad (11)$$

$$mass\ flow\ rate\ of\ air/second = \rho\ .A\ .V \quad (12)$$

The amount of power transferred to a wind turbine P_{Twind} is directly proportional to the area swept out by the rotor, the cubic power of the wind speed and the air density [11], as given in the Equation (13).

$$P_{Twind} = \frac{1}{2}\ \rho A V^3 \quad (13)$$

The power extracted from the wind by the rotor blades is the difference between the downstream and upstream wind powers. Using the Equation (11), the output power of the wind turbine is expressed as

$$P_0 = \frac{1}{2}\ mass\ flow\ rate\ /\ second\ \ (V_u - V_d{}^2) \quad (14)$$

Where, P_0 is the turbine output power, V_u is the upstream wind velocity and V_d is the downstream wind velocity. The mechanical power extracted by the rotor driving the electrical generator, is given as,

$$P_0 = \frac{1}{2}\ \rho\ A\ \frac{(V_u + V_d)}{2}\ (V_u{}^2 - V_d{}^2) \quad (15)$$

The output power characteristics can be assumed that, it starts generating at the cut in wind speed V_C. The output power increases linearly as the wind speed increases from V_C. The rated power P_R is produced when the wind speed varies from V_R to cut-out wind speed V_F. The output power of the wind power system P_W is expressed as

$$P_w = \begin{cases} P_R \cdot \frac{V - V_c}{V_R - V_c} & \text{for } V_C \le V \le V_R \\ P_R & \text{for } V_R \le V \le V_F \\ 0 & \text{for } V < V_c \text{ or } V > V_F \end{cases} \quad (16)$$

Where, V_C is the cut-in wind speed V_R is the rated wind speed and V_F is the cut-out wind speed. In this, all Equations describe the output power and torque of the wind turbine and constitute the turbine model. The Matlab/Simulink implementation of the turbine model is shown in Fig. 5.

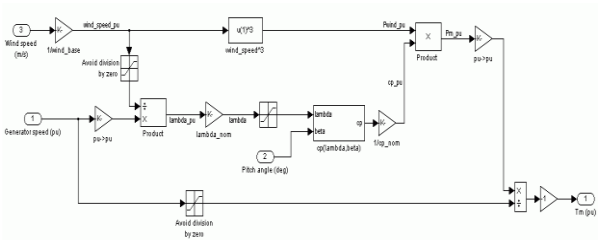

Figure 5. Simulated model of wind turbine

4.2 PMSG Model

The Permanent Magnet Synchronous Generator (PMSG) differs from the induction generator in that the magnetization is provided by a permanent magnet pole system featuring to provide the self-excitation. The self-excitation allows the operation of PMSG at high power factors and high efficiency [12]. A PMSG connected to the DC-link of the series connected VSI of the SAF via a power electronic converter configuration is utilized for variable speed wind system. Power electronic converter converts the variable frequency, variable voltage output of the generator into a fixed DC voltage to make it suitable for the DC-link of the VSI. A simple configuration of a variable speed wind system with PMSG machine is shown in Fig. 6.

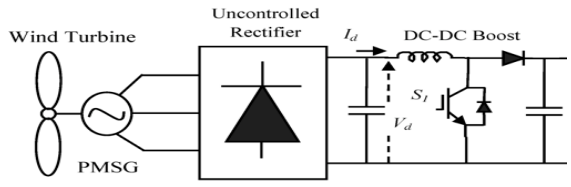

Figure 6. Variable speed wind system with PMSG machine

In the PMSG model, the flux is assumed to be sinusoidally distributed along the air gap. The mathematical equations are constructed by aligning the d-component of machine vector to the rotor flux. Voltage equations of the machine have the following forms:

$$v_{sd}^r = R_{st} i_{sd}^r - \omega_r \psi_{sq}^r + \frac{d\psi_{sd}^r}{dt} \quad (17)$$

$$v_{sq}^r = R_{st} i_{sq}^r - \omega_r \psi_{sd}^r + \frac{d\psi_{sq}^r}{dt} \quad (18)$$

The d-axis and q-axis components of stator flux ψ_{sd}^r and ψ_{sq}^r are obtained from the following equations

$$\psi_{sd}^r = X_{sd} i_{sd}^r + \psi_{pm}^r \quad (19)$$

$$\psi_{sq}^r = X_{sq} i_{sq}^r \quad (20)$$

where, v_{sd}^r is the d-axis component of the terminal voltage vector, v_{sq}^r is the q-axis component of the terminal voltage vector, i_{sd}^r is the d-axis component of the stator current, i_{sq}^r is the q-axis component of the stator current, R_{st} is the stator resistance, X_{sd} is the d-axis component of the stator reactance, X_{sq} is the q-axis component of the stator reactance and ψ_{pm}^r is the permanent magnet flux linkage. The electromagnetic torque T_e of PMSG can be expressed as

$$T_e = i_{sq}^r (i_{sd}^r \ X_{sd} - X_{sq} \ + \psi_{pm}^r) \quad (21)$$

4.3 DC-DC Boost Converter

The varying nature of the output power and voltage of the wind energy conversion system requires a converter to regulate the output voltage. The power electronic converters are becoming more attractive in improving the performance of wind power generation systems. DC-DC boost converter can be used as switching mode regulators to convert an unregulated DC voltage to a regulated DC output voltage. The regulation is normally achieved by PWM technique at a fixed frequency. The wind generation systems are connected to individual DC-DC boost converters and the outputs of the DC-DC boost converters are then connected to a DC-link of three-phase VSI. The basic structure and control topology of the proposed DC-DC boost converter are illustrated in Fig. 7. Control voltage V_c is obtained by comparing the actual output voltage of the converter with its desired value V_{ref}. V_c can be compared with a sawtooth waveform via a relational operator or a comparator to generate the PWM control signals for the DC-DC boost converter. The DC-DC boost converters can be operated in two modes: 1) Continuous Conduction Mode (CCM) and 2) Discontinuous Conduction Mode (DCM). The CCM mode of operation is more efficient for power conversion than the DCM mode of operation. Hence, CCM mode of operation is utilized here to regulate the output voltage of the wind system. When the switch S is ON, the diode D is reverse biased by switch S and V_{co}, thus isolating the output stage. The input current i_s, which raises linearly, flows through inductor L_s and switch S. The input voltage V_{in} supplies the energy to the inductor during the ON period T_{on} [13]. The voltage across the inductor V_{Ls} is given as,

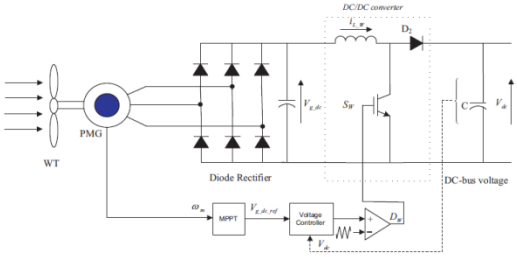

Figure 7. Circuit diagram of DC-DC boost converter

$$V_{L_s} = L_s \frac{di_s}{dt} \quad (22)$$

$$V_S = V_{L_s} \quad (23)$$

$$V_{L_s} = i_s X_{L_s} \quad (24)$$

Where, X_{L_s} is the reactance of the inductor L_s and V_{in} is the input source voltage in V. When the switch S is OFF, the inductor current is forced to flow through the diode D and load for a period T_{off}. As the current tends to decrease,

polarity of the emf induced in inductor L_s is reversed. It is connected in series with voltage source V_{in} and load through diode D. The inductor current decreases until the switch S is turned ON again. The output voltage V_o is expressed as,

$$V_0 = V_{in} + L_s \frac{di_s}{dt} \quad (25)$$

The average output voltage of the DC-DC boost converter is given as

$$V_0 = \frac{V_{in}}{1-D} \quad (26)$$

and D is given by, $$D = \frac{T_{on}}{T_{on}+T_{off}} \quad (27)$$

Where, D is the Duty Cycle in %, T_{on} is the ON time in sec and T_{off} is the OFF time in sec. The output voltage V_o is inversely proportional to 1-D. It is obvious, that the duty cycle D should not be equal to 1 [14].

4.4 Maximum Power Point Tracking Control

The MPPT is an essential part of a wind solar system. This is designed to automatically find the maximum power point of the wind. In this paper, a dc-dc converter with P&O MPPT algorithm based on fuzzy controller is incorporated to track the maximum power point of the wind system.

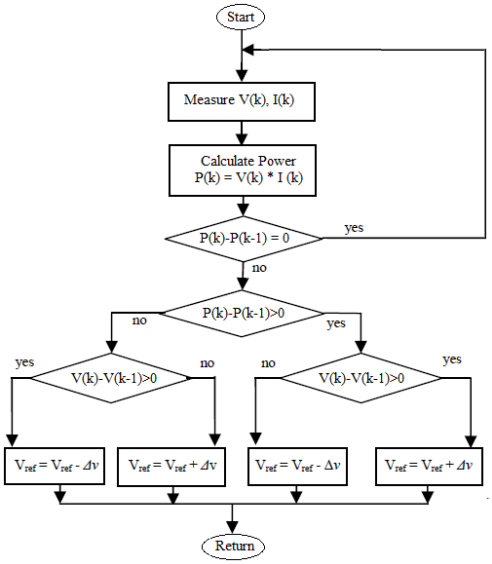

Figure 8. Flow chart of P&O MPPT algorithm

The P&O MPPT algorithm applies a small increment or decrement of perturb voltage ΔV to the wind system operating voltage. The inputs of fuzzy controller are measured from the output of wind system to generate control signal (V_{ref}) for the PWM generator. The flow of P&O MPPT algorithm is shown in Fig.8. The principle of operation of the P&O MPPT is presented in [15].

The computation of actual state (k) and previous state (k-1) of the parameters V and I are considered. The actual and previous state of the power is calculated from the product of actual and previous state V and I as shown in Fig.9. According to the condition as represented in Fig.9, the increment or decrement of reference voltage (V_{ref}) of the PWM pulse generator is obtained. The simulink block diagram of the fuzzy controller based P&O MPPT is shown in Fig. 9.

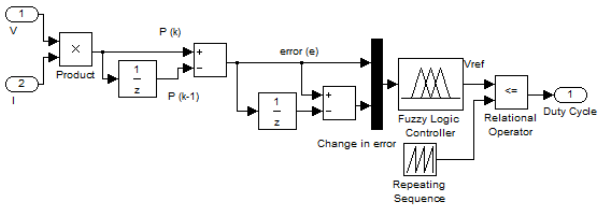

Figure 9. Control structure of fuzzy MPPT

The inputs and output of fuzzy controller are expressed as a set of linguistics variables as follows: NB-Negative Big, NS-Negative Small, ZE-Zero, PS-Positive Small and PB-Positive Big. The output of the fuzzy is chosen form a set of semantic rules that lead to track the maximum power point of PV array. The set of rules chosen are shown in Table 4.

Table 4 Fuzzy rules for mppt method

e/ce	**NB**	**NS**	**ZE**	**PS**	**PB**
NB	ZE	ZE	PB	PB	PB
NS	ZE	ZE	PS	PS	PS
ZE	PS	ZE	ZE	ZE	NS
PS	NS	NS	NS	ZE	ZE
PB	NB	NB	NB	ZE	ZE

5. W-SAF Controller

The control system of SAF with fuzzy controller is shown in Fig.10.This compensator solves harmonic problems in the source side. In the conventional controllers like P, PI and PID, the control parameters are fixed at the time of design. Hence, the conventional controllers offer good performance only for the linear system. When the operating point of the system is changed, the parameters of the conventional controllers should be designed again, and some trials and prior information of the systems are needed to design the parameters. The fuzzy controller overcomes the drawbacks of the conventional controllers [16-17]. In this method, the measured three phase supply voltage (V_{abc}, I_{abc}) is converted to rotating reference frame I_d and I_q using the angle obtained from the discrete 3 phase PLL.

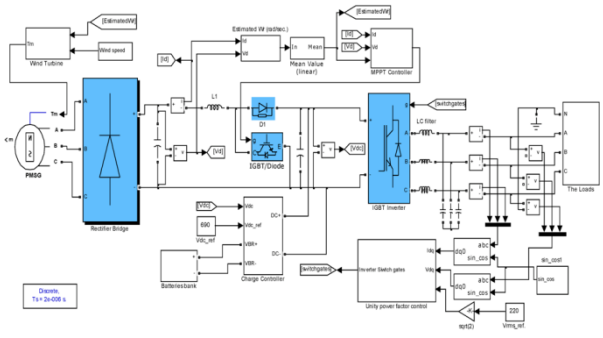

Figure 10. Control system of SAF

During transient, the dc value of V_d is dropped/raised from its nominal value and difference between the reference voltage $V_{ref\ (pu)}$ and $|V_s|$ form an error signal. The error and change in error signals are the two inputs of fuzzy controller. The processed error signal is then converted back to $V_{abc(ref)}$ through a dq to V_{abc} transformation, which is then modulated using Sinusoidal Pulse Width Modulation (SPWM) to produce the required pulse to switch on the three phase inverter, thus restoring the load voltage. The basic idea of SPWM is to compare a sinusoidal control signal $V_{abc(ref)}$ of normal frequency 50 Hz with a triangular carrier waveform $V_{carrier}$ with 20 kHz signal to produce the PWM pulses for three phase SAF. When the control signal is greater than the carrier signal, the switches are turned on, and their counter switches are turned off. The output voltage of the inverter mitigates harmonics.

The fuzzy controller has two inputs, name by error and change in error and one output. The error and change in error are defined as

$$e\ (error) = V_{ref} - V_s \tag{28}$$

$$ce\ \ change\ in\ error = e\ n - e\ n-1 \tag{29}$$

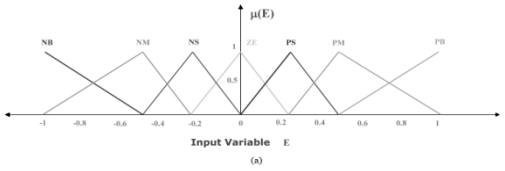

Figure 11a Membership function for input variable "error"

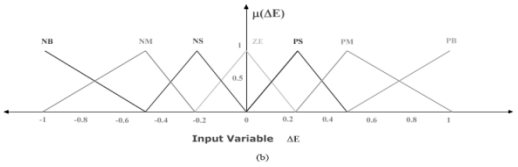

Figure 11b Membership function for input "change in error"

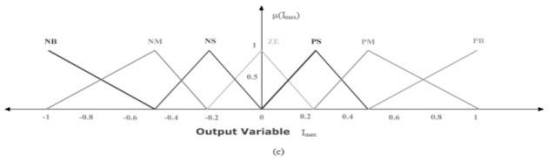

Figure 11c Membership function for output variable "output"

The membership functions of the error, change in error and output variables are shown in Fig.11a, Fig.11b and 11c. The membership functions are triangular shaped with 50% overlap for a precise control.

Table 5 Fuzzy Rules For Saf Control

e/c**e**	**NB**	**NM**	**NS**	**ZE**	**PS**	**PM**	**PB**
NB	PB	PB	PB	PM	PM	PS	ZE
NM	PB	PB	PM	PM	PS	ZE	NS
NS	PB	PM	PM	PS	ZE	NS	NM
ZE	PM	PM	PS	ZE	NS	NM	NM
PS	PM	PS	ZE	NS	NM	NM	NB
PM	PS	ZE	NS	NM	NM	NB	NB
PB	ZE	NS	NM	NM	NB	NB	NB

where, the inputs and output linguistic variables called fuzzy sets are labeled as follows: NB-Negative Big, NM-Negative Medium, NS-Negative Small, S-Small, PS-Positive Small, PM-Positive Medium, PB-Positive Big, NB-Negative Big, NM-Negative Medium, NS-Negative Small, ZE-Zero, PS-Positive Small, PM-Positive Medium and PB-Positive Big. The input signals are fuzzified and represented in fuzzy set notations by membership functions. The defined 'if and then' rules produce the linguistic variables and these variables are defuzzified into control signals to generate PWM gating pulses for VSI. There are 49 rules, utilized to produce the optimum control signal. The fuzzy rules used for simulation are shown in Table 5.

6. Simulation Results Discussion

The performance of the proposed W-SAF discussed under two cases A: balanced, unbalanced load and case B: energy conservation. For these cases, the system frequency is maintained at 50 Hz and sample time is chosen to be 50 μsec. In each case, the total period of simulation is carried out for 0.35 sec.

Table 6. Specifications for W-SAF simulated system

Description	**Parameter**	**Value**
AC Supply	Line Voltage	400 V
	Frequency	50 Hz
Filter	Filter Inductance	38 mH
	Filter Capacitance	20 μF
DC Bus	Voltage	680 V
Load	Load Resistance	120 Ω
	Load Inductance	0.5 mH
Battery Bank	Nominal Voltage	300 V
	Capacity	400 Ah
DC-DC Boost Converter	Inductance	18.33 μH
	Switching Frequency	25 kHz
Wind Turbine	Rated Power	1000 W
	Rated Voltage	96 V
	Rotation Speed	330 RPM
	Start-upWind Speed	2.5 m/s

The input voltage of 400 V three-phase AC supply is given to load through three-phase programmable AC source. The switched-mode PWM VSI is made to operate at 180^0 conduction mode. This mode of operation is used to minimize the shoot through fault between two switches in the same leg. The supply voltage, source current and injected current of the proposed SAF are measured using the three individual scopes. Three-phase VSI is operated by six gate pulses generated from the PWM pulse generator. The PWM generator has pulse amplitude of 1 V for all the six pulses. The system parameters considered for the analysis of the proposed W-SAF are furnished in Table 6.

6.1 Balanced Load and Unbalanced Load

Initial investigation is started to analysis the performance of the proposed system under balanced and unbalanced load condition, the harmonic current detection block detects the

variation of the supply current as soon as it occurs and it generates the actuating signal to activate the PWM pulse generator. Input source voltage as shown in Fig. 12a. The SAF responds to inject the compensating current (as shown in Fig.12c.) in shunt with the supply to restore the source current at nominal level as shown in Fig.12d. The supply current is the sum of load current and injected SAF output current. During the initial period, there is no load deviation in the load from 0 and 0.1 s as shown in Fig.12b. Hence, the programmable three-phase AC voltage source feeds the total active power of 1000 W to the load.

During the transient, three-phase load is reduced to two phase between 0.1 and 0.2s. The load is changed to two phase load and also the load currents are absence between 0.2 s and 0.25 s. These loads are applied again at 0.25 s respectively as shown in Fig.12b. From Fig.12c. It's observed that the non linear load injects harmonics in the supply. It reduces the supplied active power of source from 1000 W to 520 W. The proposed SAF responds to the current transient and injects the missing active power during the period 0.1 sec to 0.2 sec as shown in Fig. 12i. The resultant active power of the load oscillates at 0.1 sec and it stabilizes at 0.13 sec. During the period of current, the reactive power supplied by the source is reduced from 600 VAR to 210 VAR as illustrated in Fig. 12i.

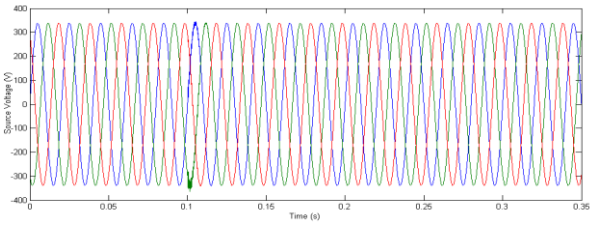

Figure 12a. Source voltage.

The SAF responds to the current transient and injects a reactive power of 400 VAR to restore the reactive power of load. The instantaneous THD contents of three-phase load current for Case A is obtained through FFT analysis and shown in Fig. 12g. From Fig. 12e and 12f, Shows the neutral current compensation before and after the SAF control strategy implementation. After the SAF compensation source current maintain inphase with the voltage as shown in Fig. 12h.

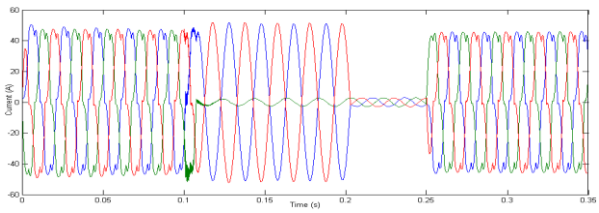

Figure 12b. load current without compensation.

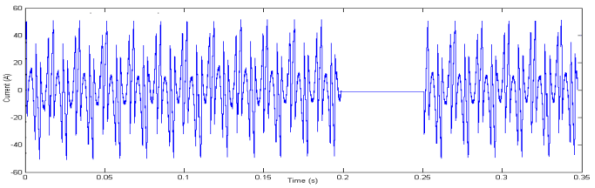

Figure 12c. Injected current for compensation.

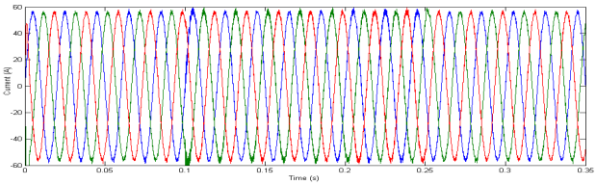

Figure 12d. Source current after compensation.

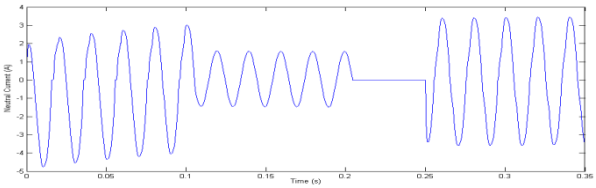

Figure 12e. Neutral current without compensation.

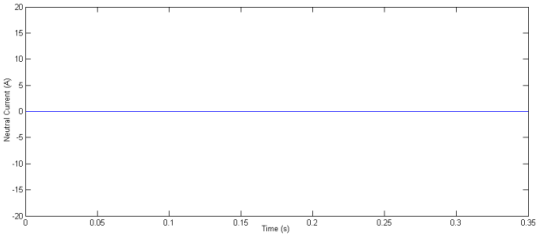

Figure 12f. Neutral current after compensation.

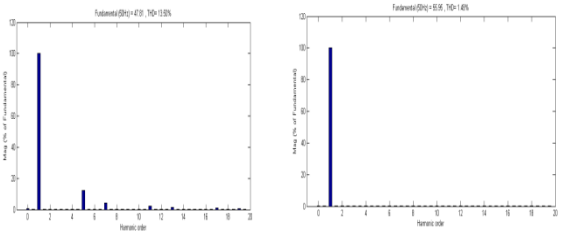

Figure 12g. (a) before and (b) after compensation.

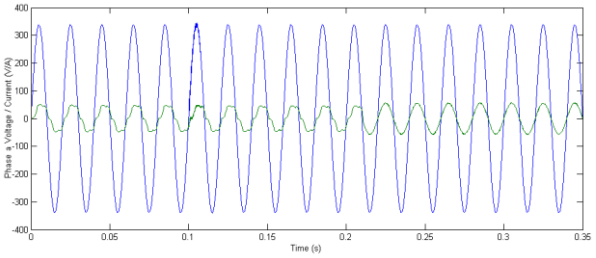

Figure 12h. Source voltage & current after compensation.

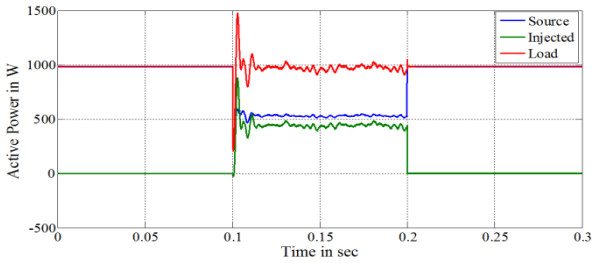

Figure 12i. Source, injected and load reactive power

6.2 Energy Conservation

In this case is made to show the performance of the W-SAF in conserving the energy consumption from the utility grid. In order to determine the performance of the SAF in reducing the energy consumption of the utility distribution system, power generation on the wind system is simulated.

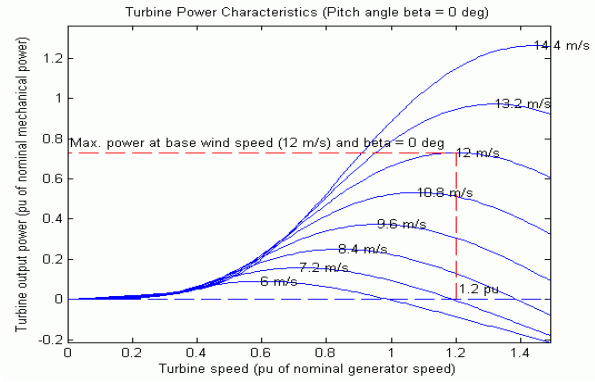

Figure 13. Mechanical output power of wind turbine

When, the wind system generates excessive power than the load demand, the energy conservation mode of the W-SAF is activated. As soon as excessive power generation on the wind system is detected, the proposed SAF disconnects the utility grid from the load. The excessive power generated on the wind system is directly feed to the load. Batteries accumulate the excessive power generated by the wind system and store it for future use. The mechanical output power characteristic of the selected wind turbine is shown in Fig. 13. From the Fig.13. It is observed that the modeled turbine can produce 0.9 p.u of mechanical power at 10 m/s of wind speed. To check the feasibility of the proposed wind system, the investigation is carried out for the wind speed of 5 m/s during 0 sec to 0.15 sec and the second is carried out for 10 m/s during the period of 0.15 sec and 0.3 sec.

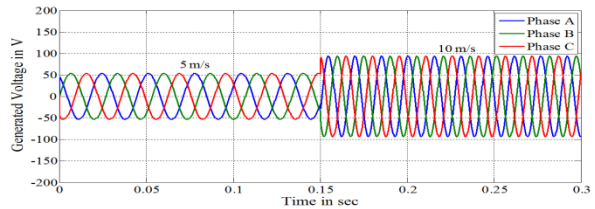

Figure 14a. Generated voltage of PMSG with varying speed

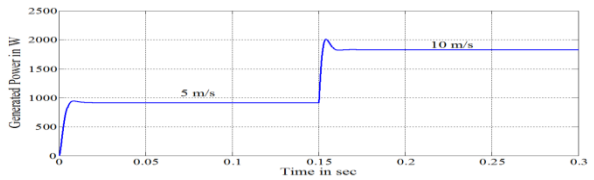

Figure 14b. Generated power of PMSG with varying speed

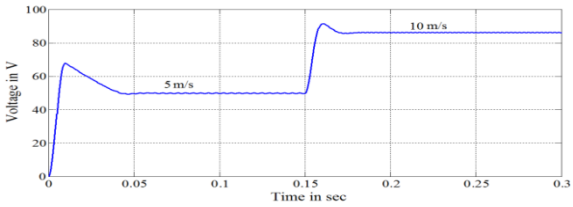

Figure 14c. Output of the rectifier with varying input voltage

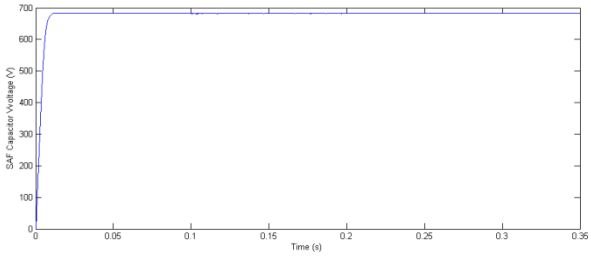

Figure 15.Output of DC-DC converter

The generated three-phase voltage and power of the PMSG with varying wind speed are shown in Figures 14a and 14b, respectively. The output voltage of the PMSG as shown in Fig.14c is fed to three-phase rectifier for AC to DC conversion and then the rectified output of the three-phase rectifier fed to DC-DC boost converter. The DC-DC boost converter regulates the output voltage at 700 V. The output voltage of the rectifier and regulated output of DC-DC boost converter are shown in Fig.15.

From the Figures 14b, it is found that the generated power on the wind system is greater than the load demand. The SAF detects the power generation and responds to the excessive power generation by disconnecting the utility grid from the load. The wind system can tackle the total load power demand of 1160 W. The remaining power is utilized to charge the battery bank. When the power generation on the wind system is lower than the load demand, then the coordinating logic presented in the Table 2, connects the output of the three-phase rectifier in parallel with the output of the wind system to manage the load demand. The RMS value of the supply voltage, injected voltage and load voltage of the SAF are shown in Fig. 16. In this case, the SAF injects the nominal voltage of 400 V in parallel with the load. On examining the results, it is found that the proposed SAF is able to conserve the energy. This case provides an additional financial benefit to the users by reducing the power consumption from the utility grid. The active and reactive powers of the SAF for Case B are shown in Fig. 17 and Fig. 18, respectively. In this case, the SAF injects an active power of 1000 W and reactive power of 600 VAR to the load.

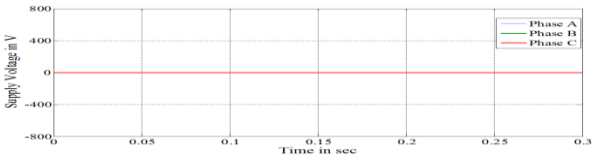

(a) Supply voltage

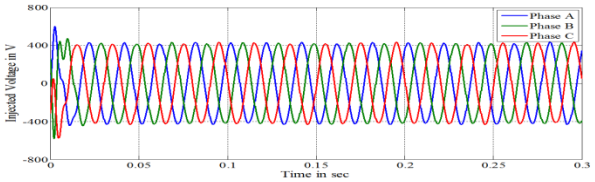

(b) Injected voltage

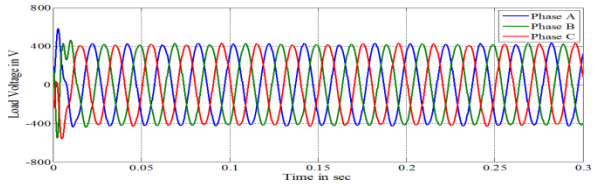

(c) Load voltage

Figure 16. Supply injected and load voltage of W-SAF

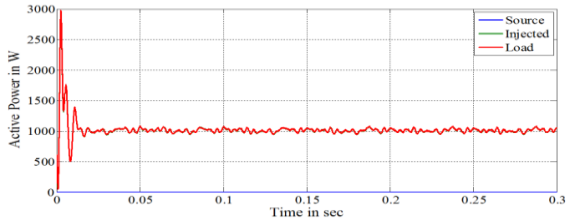

Figure 17. Source, injected and load active power of W-SAF

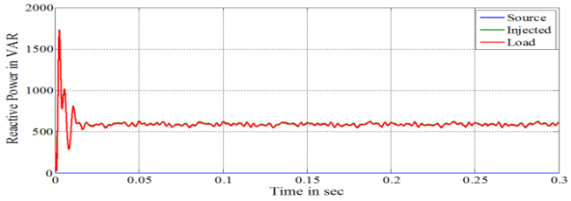

Figure 18. Source, injected & load reactive power of W-SAF

The FFT analysis has been carried out for the load voltages to determine the THD, which is illustrated in the Fig. 19. The THD value of phase A, phase B and phase C are 0.56%, 0.63% and 0.40%, respectively, which are less than 5%. The THD values of phase A, phase B and phase C are very minimum and lies within the permissible limits.

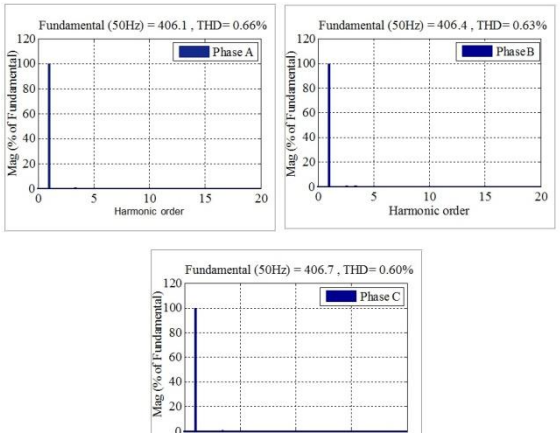

Figure 19. THD contents of the three-phase load voltage

7. Conclusion

This paper presents a novel application of utilizing a wind system as SAF for harmonic mitigation, reactive power compensation and neutral current compensation at the point of common coupling (PCC) at a small industry. A dc-dc converter with fuzzy controller based P&O MPPT algorithm is implemented to track the maximum power point of the wind turbine. A fast convergence with small oscillation at the maximum power point can be achieved by this method. This novel W-SAF can reduce the energy consumption from the three phase utility grid, when the wind system generates excessive power or equal power to the load demand. Further, it reduces the energy consumption tariff and avoids the use of stabilizer for the individual equipment at a residence, small industry, etc. The simulation results show that the W-SAF performance is satisfactory in mitigating the current variations.

8. References

[1]. Akagi H, Kanazawa Y, Instantaneous (1984). Reactive Power Compensators Comprising Switching Devices without Energy Storage Components. IEEE Transactions on Industry Applications. 20(3): 625-630.

[2]. Peng Z (1998). Harmonic and Reactive Power Compensation Based on the Generalized Instantaneous Reactive Power Theory for Three-Phase Four-Wire Systems. IEEE Transactions on Power Electronics. 13(5): 1174-1181.

[3]. Montero M I M (2007). Comparison of Control Strategies for Shunt Active Power Filters in Three-Phase Four-Wire Systems. IEEE Transactions on Power Electronics. 22(1): 229-236.

[4]. Vodyakho O, Chris Mi Senior C (2009). Three-Level Inverter-Based Shunt Active Power Filter in Three-Phase Three-Wire and Four-Wire Systems. IEEE Transactions on Power Electronics. 24(5): 1350- 1363.

[5]. Aredes M (1997). Three-Phase Four-Wire Shunt Active Filter Control Strategies. IEEE Transactions on Power Electronics.12(2): 311-318.

[6]. Akagi (2007). Instantaneous Power Theory and Applications to Power Conditioning. IEEE Press/Wiley-Inter- Science

[7]. Mikkili S, Panda A K (2011). Instantaneous Active and Reactive Power and Current Strategies for Current Harmonics Cancellation in 3-ph 4Wire SHAF with Both PI and Fuzzy Controllers. Journal of Energy and Power Engineering. 3(3): 285-298.

[8]. Salmeron P, Herrera R S (2006). Distorted and Unbalanced Systems Compensation within Instantaneous Reactive Power

Framework. IEEE Transactions on Power Delivery. 21(3): 1655-1662.
[9]. Mikkili S, Panda A K (2011). SHAF for Mitigation of Current Harmonics Using p-q Method with PI and Fuzzy Controllers. Engineering, Technology & Applied Science Research, 1(4): 98-104.
[10]. Patel, M.R. (1999) "Wind and solar power systems: Design, Analysis and Operation", Second Edition, CRC Press LLC, N.W. Corporate Blvd., Boca Raton, Florid.
[11]. Johnson, G.L. "Wind Energy systems", England Cliffs: Prentice-Hall, 2001.
[12]. Gieras, J. and Wing, M (2002) "Permanent Magnet Motor Technology: Design and Applications", Second Edition, CRC Press LLC, N.W. Corporate Blvd., Boca Raton, Florida.
[13]. Mohan, N., Undeland, T.M. and Robbins, W.P. (2006) "Power Electronics Converters: Applications and Design", Third Edition, Jhon Wiley & Sons Asia Pte. Ltd., Singapore:172-178,
[14]. Rashid, M.H. (2203). "Power Electronics Circuits, Devices and Applications," Second Edition, Prentice-Hall of India Private Ltd, New Delhi.
[15]. Elgendy, M.A., Zahawi, B. and Atkinson D.J. (2012), "Assessment of perturb and observe MPPT algorithm implementation techniques for PV pumping applications", IEEE Transaction on Sustainable Energy, 3(1): 21-33,
[16]. Jain S K (2002). Fuzzy Logic Controlled Shunt Active Power Filter for Power Quality Improvement. IEEE Proceedings Electric Power Applications. 149(5):317-328.
[17]. Kirawanich P, O'Connell RM (2004). Fuzzy Logic Control of an Active Power Line Conditioner. IEEE Trans-actions on Power Electronics.19(6):1574-1585.

G.Vijayakumar received his bachelor degree in Electrical and Electronics Engineering from Mahendra engineering college, Namakkal in 2003.He received his Master degree in Power Electronics and Drives from Bannari Amman institute of technology, Sathyamangalam under the Anna University, Chennai, in 2007 and he received his doctorate degree from Anna University, Chennai in the area of Power Systems. he has published more than 12 research papers in reputed National and International journals. Currently he is working as an Assistant Professor in K.S.R. College of Engineering, Tiruchengode, Namakkal. He is a life member in ISTE. His research interests are in the areas of Grid interfaced renewable energy sources, Power quality and hybrid filter for harmonic compensation.

C.Karthikeyan, Tiruchengode, Namakkal, Tamilnadu, India. He received the B.E. and M.E degrees, from Bharathiar University, Coimbatore, TN, India and Anna University, Chennai, TN, India. in 2001 and 2005, respectively. After he was worked as a Lecturer in the Department of Electrical and Electronics Engineering (from June 2001) in Kaavery Polytechnic College, Salem, TN, and India. He was worked as a Lecturer (from 2005) in the Department of Electrical and Electronics Engineering in MPNMJ Engineering College, Erode, TN, India. (affiliated to Anna University of Technology, Coimbatore) and He was worked as a Lecturer (from 2007) and as a Assistant Professor (from 2008) in the Department of Electrical and Electronics Engineering in K.S.R. College Engineering College, Tiruchengode, Namakkal, TN, India. (affiliated to Anna of Technology, Coimbatore) and he has been working as a Associate Professor in the Electrical and Electronics Engineering at K.S.R. College of Engineering (affiliated to Anna of Technology, Coimbatore)since June 2010. His research interest includes Electro Magnetic Interference mitigation in Inverter & Optimal switching angles for reduction of Harmonics in Inverter. Other areas include Genetic Algorithm and Artificial Neural Network. He is a member of ISTE.

V. Ravi received the B.E. and M.E degrees, from Periyar Univ. and Annamalai Univ. in 2002 and 2004 respectively. After working as a Lecturer (from 2004) in the Dept. of Electrical and Electronics Engineering in MPNMJ Engineering College, Erode, India - affiliated to Anna Univ. and as a Lecturer (from 2007) and as a Assistant Professor (from 2008) in the Dept. of Electrical and Electronics Engineering in K.S.R. College Engineering College, Tiruchengode, India - affiliated to Anna Univ. and he has been working as a Associate Professor in the Dept. of Electrical and Electronics Engineering at K.S.R. College of Engineering, Tiruchengode, India - affiliated to Anna Univ. since June 2010. His area of interest includes Power Systems. He is a member of ISTE.